CHEMISTRY
A European Journal

Supporting Information

Complex Reaction Environments and Competing Reaction Mechanisms in Zeolite Catalysis: Insights from Advanced Molecular Dynamics

Kristof De Wispelaere,[a, b] Bernd Ensing,*[b] An Ghysels,[a] Evert Jan Meijer,[b] and Veronique Van Speybroeck*[a]

chem_201500473_sm_miscellaneous_information.pdf

Supporting Information

Contents

S1. Unit cell for H-SAPO-34

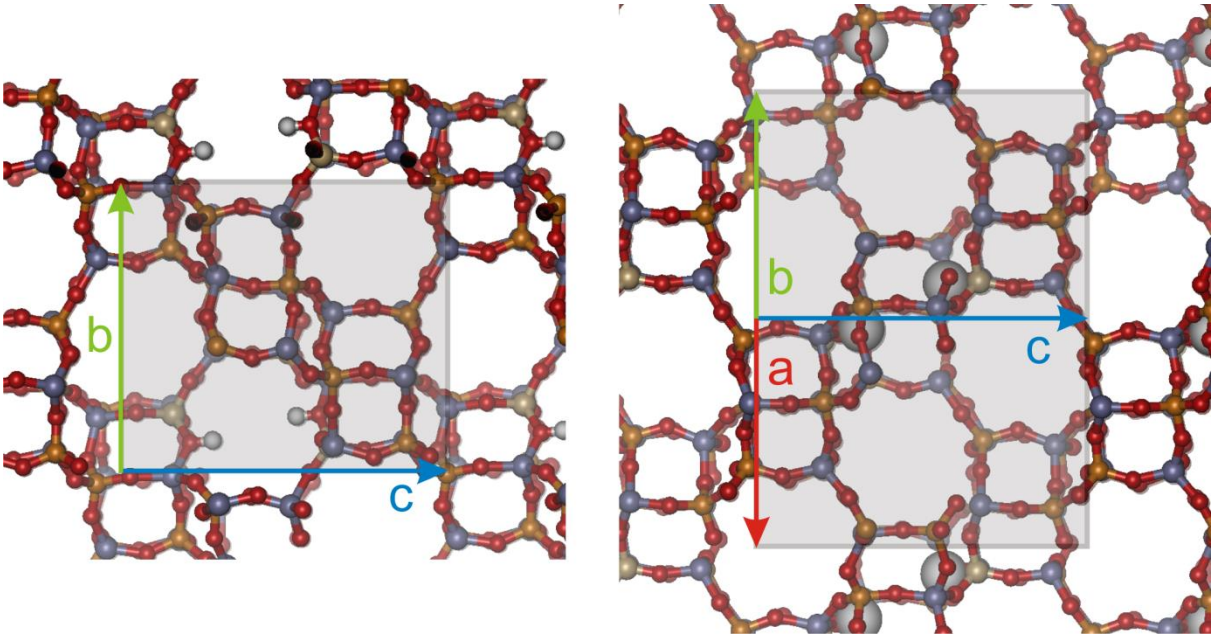

Figure S1.1. Unit cell of H-SAPO-34 (grey box), with indication of the two acid sites, located in the 8-ring connecting two chabazite cages. Left: seen along the a axis. Right: seen along a direction, making an angle of 60° with the a axis and b axis.

The positions of the acid sites correspond with those chosen in earlier work of the present authors.[1-5] Note that every unit cell contains two acid sites, located in the same 8-ring. This choice was inspired by the fact that in SAPO materials it is probable to find two Si atoms in next-nearest-neighbor positions in the same 8-ring.[6, 7]

No large angle deformations were observed during the NPT simulations of the H-SAPO-34 framework loaded with different amounts of methanol or water. Therefore, the average cell lengths (a,b,c) were systematically rescaled such that $\alpha = \beta = 90°$, $\gamma = 120°$ and the volume V (= a*b*cos(30°)*c) equals the average volume from the entire MD simulation.

Table S1.1. Time-averaged cell parameters of the H-SAPO-34 unit cell loaded with different amounts of methanol or water at 350 °C.

		a [Å]	b [Å]	c [Å]	α [°]	β [°]	γ [°]
MeOH	1	14.06797	14.09985	14.8673	90	90	120
	3	14.07047	14.07058	14.95435	90	90	120
	4	14.0165	14.08226	15.03817	90	90	120
	5	14.02043	14.07993	15.1254	90	90	120
H_2O	1	14.08932	14.13206	14.76261	90	90	120
	4	14.09168	14.09533	14.71269	90	90	120
	5	14.09930	14.06693	14.26806	90	90	120
	6	14.10441	14.10104	14.42585	90	90	120
	7	14.05496	14.07756	14.96525	90	90	120
	8	14.01965	14.07727	15.00951	90	90	120

S2. Framework flexibility of H-SAPO-34 upon water or methanol adsorption

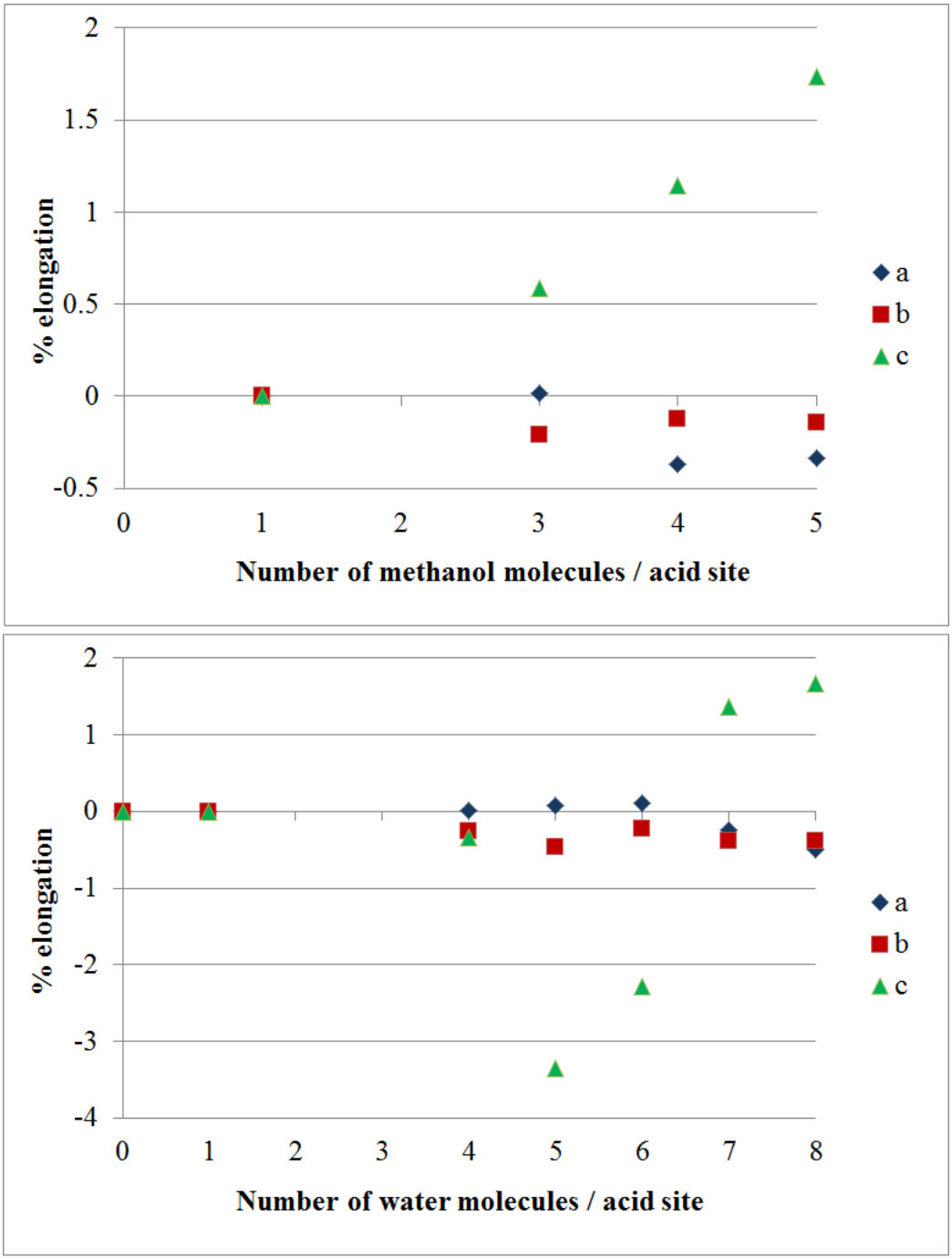

Figure S2.1. Variation of the cell lengths (a,b,c) of H-SAPO-34 with 2 acid sites per unit cell upon adsorption of different amounts of methanol (top) or water (bottom) at 350 °C.

S3. Pore filling upon adsorption of 5 methanol or 8 water molecules per acid site

To obtain a deeper understanding of the observed similarity for the framework deprotonation probability with 5 methanol or 8 water molecules per acid site, we took a snapshot of the MD simulations and displayed all atoms with their respective van der Waals spheres. Visually, a similar degree of filling of the elliptic cages, hence a similar density inside the pores is observed in both cases. The loading of guest molecules is relatively high. Nonetheless, the mobility of the guest molecules is still high enough to allow a good sampling of proton mobility.

It would also be interesting to develop models that allow detailed analysis of the structure of protic molecules in the confined environment. Inspiration may be found in models that are typically used for liquid structure.[8] This further model development is however beyond the scope of this article. It is also worth mentioning that although 5 methanol or 8 water molecules per acid site give rise to a similar probability for framework deprotonation, the hydrogen bonded clusters that are formed by water are in general larger than in methanol (see section S5).

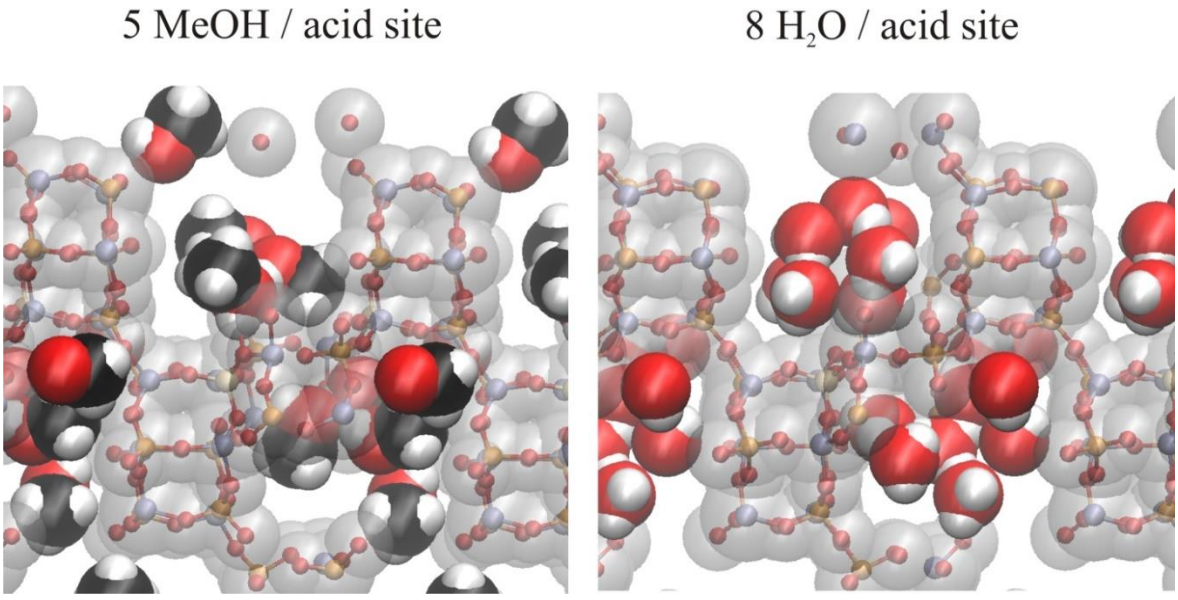

Figure S3.1. Snapshot of an MD simulation at 350 °C of H-SAPO-34 with 5 MeOH (left) or

8 H_2O (right) molecules per acid site. Van der Waals spheres are displayed for both the framework (gray, transparent) and the guest molecules and show the degree of pore filling with these loadings.

S4. Shortest distance between hydrogens/protons and acid site oxygens in H-SAPO-34

The positions of the protons and all hydrogen atoms in the system were traced during the 50 ps NPT simulations of H-SAPO-34 at 350 °C, loaded with different amounts of methanol (1,3,4 or 5 molecules per acid site) or water (1, 4, 5, 6, 7 or 8 molecules per acid site), to detect proton transfer. From the MD trajectories, the probability that at least one of the two acid sites in the unit cell of H-SAPO-34 is deprotonated was calculated. The framework is considered to be deprotonated when the shortest distance between the zeolite oxygens surrounding the substitutional defect and all hydrogen atoms exceeds 1.2 Å. The shortest distance between all hydrogens/protons (originating from methanol's hydroxyl group, water or the framework) and the two acid sites is displayed in Figure S3.1 and Figure S3.2 for the simulations with 5 methanol and 8 water molecules per acid site respectively. Apparently, the protons can be located at a reasonable distance from their original positions on the framework.

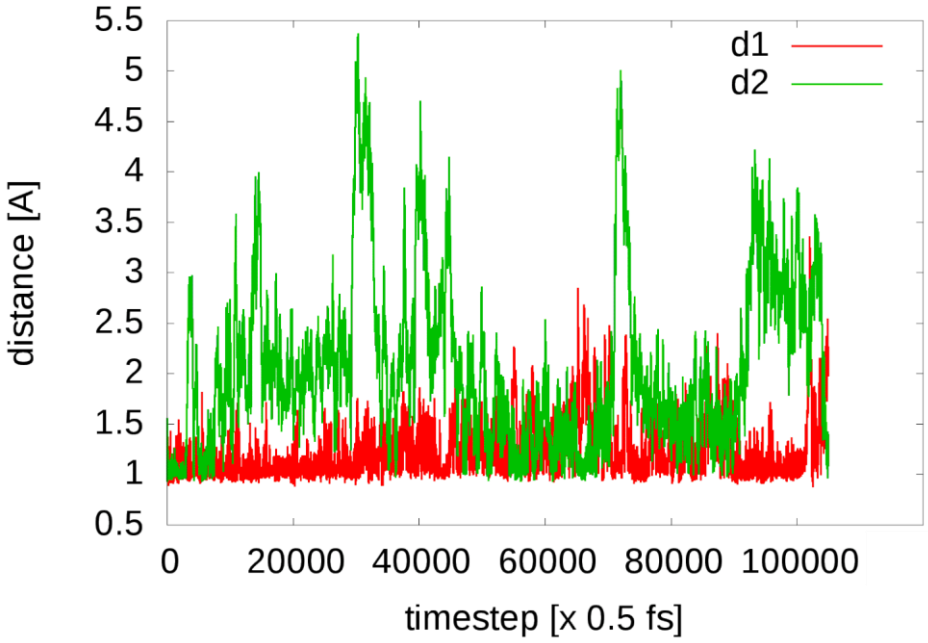

Figure S4.1. Shortest distances between all hydrogen/protons and the two acid sites in H-SAPO-34 loaded with 5 methanol molecules per acid site at 350 °C.

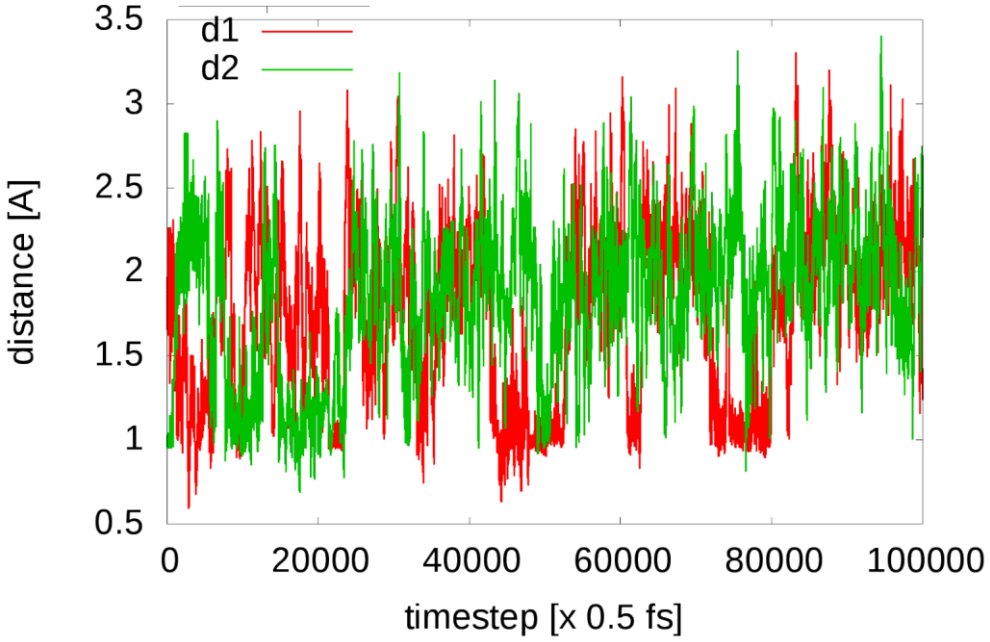

Figure S4.2. Shortest distances between all hydrogen/protons and the two acid sites in H-SAPO-34 loaded with 8 water molecules per acid site at 350 °C.

S5. Methanol and water clustering in H-SAPO-34 at 350 °C

A criterion based on an oxygen-oxygen distance with cut-off 3.5 Å and a nearly linear orientation of the O-H --- O bonds was applied to determine how large the formed hydrogen bonded methanol or water clusters are. The probability to find only single protic molecules, a dimer, trimer etc. as largest cluster in the system throughout the entire 50 ps simulation is given below.

Table S5.1. Probability for the formation of clusters of protic molecules with different sizes during an NPT MD simulation of H-SAPO-34 loaded with 5 methanol or 8 water molecules per acid site at 350 °C and 1 bar.

Cluster containing … molecules:	*5 MeOH / acid site*	*8 H_2O / acid site*
1	1 %	0 %
2	50 %	25 %
3	31 %	16 %
4	18 %	12 %
5	0 %	14 %
> 5	0 %	33 %

S6. Detailed study of proton diffusion through the 8-rings of H-SAPO-34 loaded with methanol or water

The lag time is the time between two analyzed snapshots in the simulation. A lag time of 0.1 ps for example means that only every 100 fs (or 200 time steps) a frame is selected to analyze the positions of all carbons and hydrogens in the system. 8-ring crossing can be detected, because a ring crossing is accompanied by a change in sign of ξ between subsequent trajectory snapshots. When the lag time between snapshots is taken to be longer, the number of detected ring crossings decreases because fast re-crossings make some ring crossings go unnoticed. However, even at long lag times, the number of ring crossings is sufficiently high to obtain good statistics.

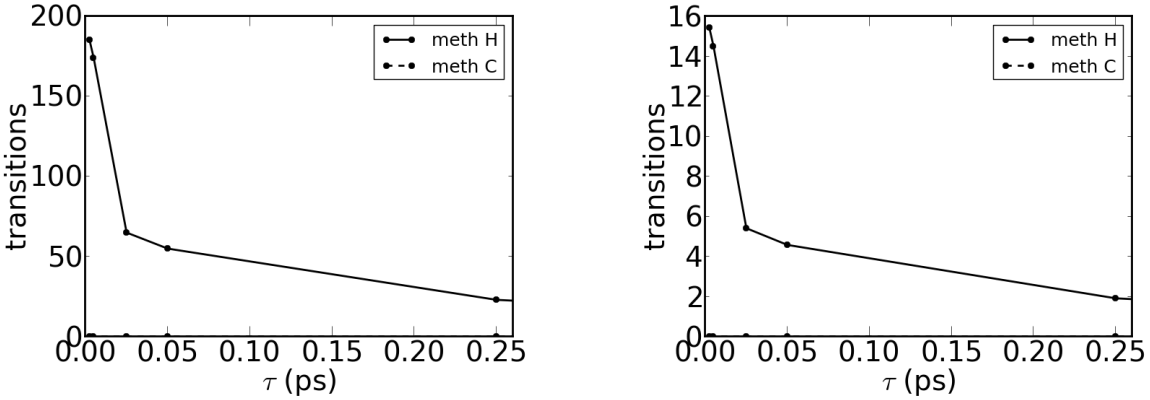

Figure S6.1. Number of sampled 8-ring transitions in terms of the lag time τ, being the time between two analyzed snapshots, during a 50 ps MD simulation of H-SAPO-34 loaded with 5 methanol molecules per acid site at 350 °C (Left: the total number of transitions; right: number of transitions per atom)

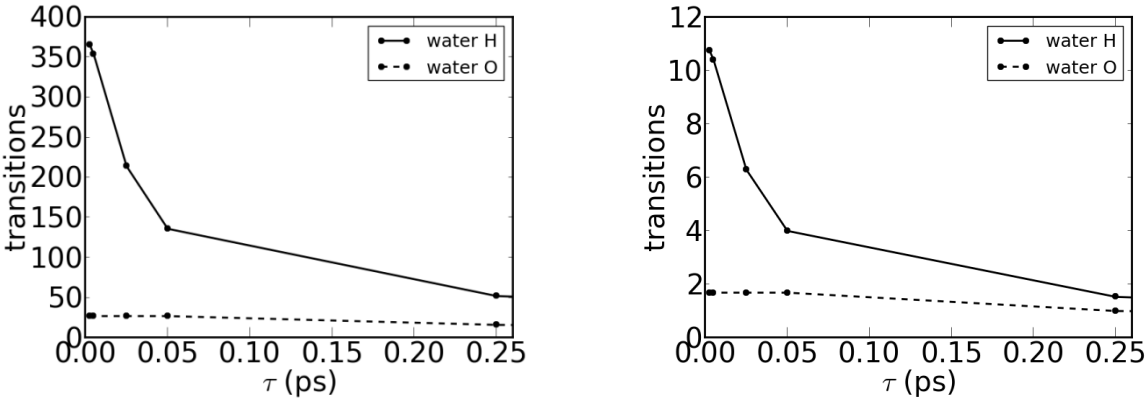

Figure S6.2. Number of sampled 8-ring transitions in terms of the lag time τ, being the time between two analyzed snapshots, during a 50 ps MD simulation of H-SAPO-34 loaded with 8 water molecules per acid site at 350 °C (Left: the total number of transitions; right: number of transitions per atom)

S7. The metadynamics approach

To enhance sampling of interesting regions on the FES, a multitude of methods has been developed,[9, 10] among which the metadynamics method, developed by Laio and Parrinello, [11-16] is very promising to study zeolite-catalyzed reactions as was earlier demonstrated by some of the present authors.[17, 18] The method relies on the choice of a limited number of collective variables along which the free energy landscape is "filled up" with gaussian-shaped bias potentials to accelerate sampling of rare events (Figure S7.1). Afterwards the sum of the gaussians can be used to reconstruct the FES.

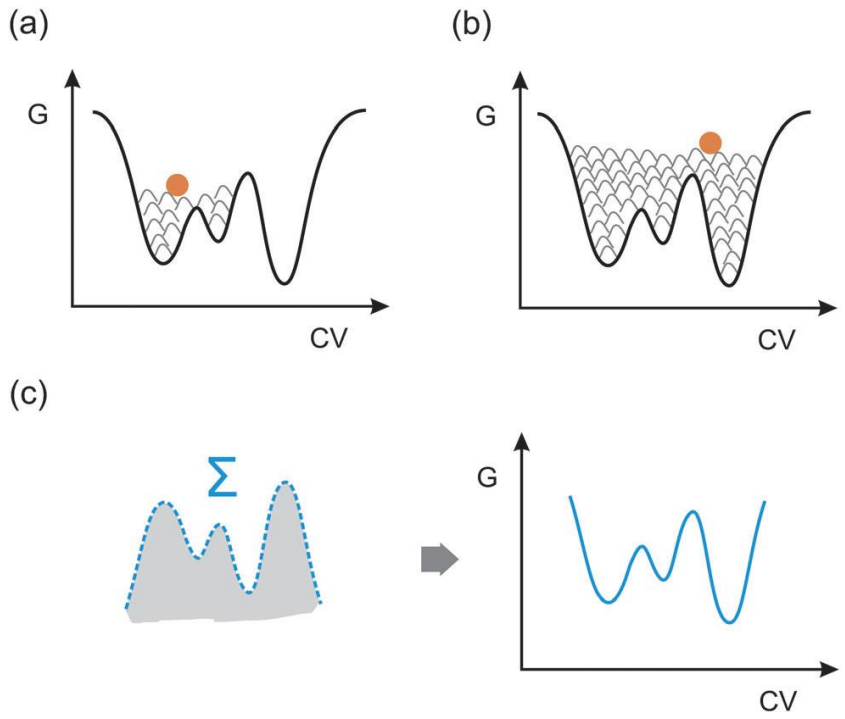

Figure S7.1. Schematic representation of the metadynamics approach.[14, 16] Free energy minima are "filled" with gaussian-shaped bias potentials or hills (a), when all minima and all transitions are sampled (b), the inverse of the sum of all gaussians yields a reconstruction of the sampled free energy surface (c). Taken from reference [19]

S8. Unit cell for H-SSZ-24

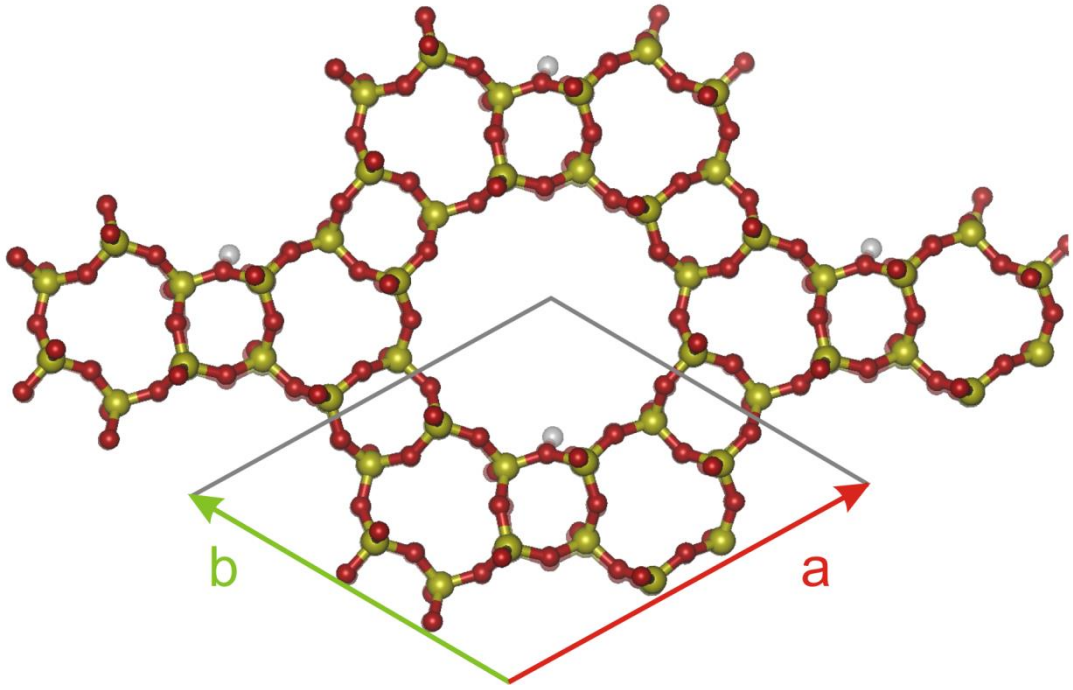

Figure S8.1. 1x1x2 super cell used for simulations with H-SSZ-24 seen along the c axis; each super cell contains 1 acid site.

For the AFI topology, there is only one possible crystallographic position for the substitutional defect. As molecular dynamics simulations are performed of the framework loaded with protic molecules (methanol), the exact location of the proton in the initial structure is not crucial. For H-SSZ-24 loaded with benzene and 2 methanol molecules at 350 °C, the time-averaged cell lengths are summarized in Table S8.1.

Table S8.1. Time-averaged cell parameters for H-SSZ-24 loaded with benzene and 2 methanol molecules at 350 °C

a	b	c	α	β	γ
13.88 Å	13.88 Å	16.81 Å	90°	90°	120°

S9. Shortest distance between hydrogens/protons and acid site oxygens in H-SSZ-24

The positions of the protons and hydrogen atoms in the system, originating from the two methanol molecules and the framework were traced during the 50 ps NPT simulations of H-SSZ24 at 350 °C and 1 bar. The framework is considered to be deprotonated when the shortest distance between the zeolite oxygens surrounding the substitutional defect and all hydrogen atoms exceeds 1.2 Å. This shortest distance is displayed in Figure S9.1. Apparently, the proton can be located at a reasonable distance – i.e. larger than typical hydrogen bond distances – from its original positions on the framework.

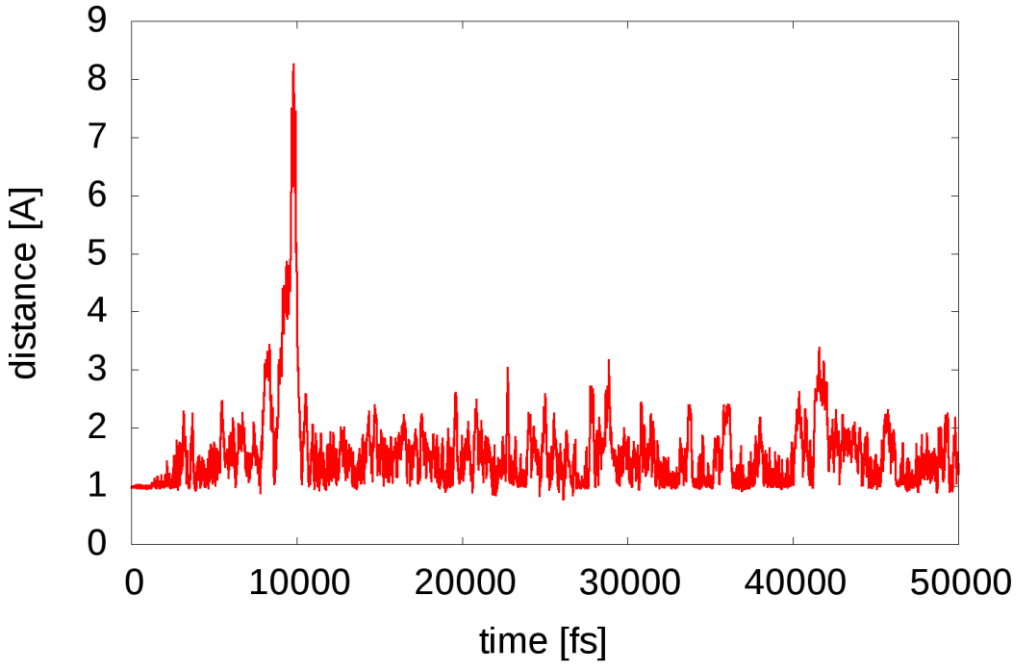

Figure S9.1. Shortest distance between all hydrogen/protons and the acid site in H-SSZ-24 loaded with 2 methanol molecules and 1 benzene molecule at 350 °C and 1 bar.

S10. Two dimensional metadynamics simulation of benzene methylation in H-SSZ-24

Initially, the methylation of benzene with 2 methanol molecules in H-SSZ-24 at 350 °C was modeled with two CVs. Imagine, one wants to study the mechanism that directly connect the reactant with the products, i.e. sample the direct methylation mechanism [20] (Figure 7a). In principle, it should be sufficient to define two collective variables to sample this reaction as was done in reference [18]: one coordination number to describe the methanol C – O bond cleavage, and one for the formation of a C – C bond between the methyl group and benzene (CN1 and CN2 in Figure 7b).

Coordination numbers CN1 and CN2, as indicated in Figure 7b, were applied to sample the direct methylation of benzene in H-SSZ-24 with 2 methanol molecules. 4400 hills were added during a 110 ps metadynamics simulation with two collective variables. Intermediate reconstructions of the resulting FES and the sampled paths are shown in Figure S10.1. During the first couple of picoseconds of the simulation (0-12.5 ps), some paths are sampled corresponding with the direct methylation (Figure S10.1 a,d). Note that these paths are located in a relatively broad region on the 2D FES, indicating that this reaction can proceed via a range of geometrically non-equivalent reaction paths. Apparently, between 12.5 and 17.5 ps, an additional free energy minimum is found, located bottom-left on the 2D free energy map (Figure S10.1 b,e). In this minimum, the methanol C – O bond is broken, but no C – C bond is formed. Visual inspection of the obtained trajectories learns that this additional free energy well corresponds with methoxides, which are known to be intermediates in the two-step methylation mechanism (Figure 7a). The formation and further reaction of these intermediate species is however not explicitly sampled as these reactions are not properly controlled by the chosen collective variables. Hence, the MTD simulation gets trapped in this minimum and a proper sampling of the direct reaction between the reactants and products is no longer possible. Moreover, the region in the (CN1,CN2)-plane corresponding with the direct

methylation (Figure S10.1 a) and the position of the additional minimum corresponding with framework bound methoxides (Figure S10.1 b,c) partially overlap. Consequently, the MTD walker cannot distinguish between the direct or the two-step mechanism and the obtained free energy profiles cannot be associated with a distinct reaction mechanism and therefore provides incomplete information. Furthermore, the approach proposed and applied in references [17] and [18] to obtain a one dimensional free energy profile from the 2D surfaces by projecting the FES on the bottom-right to top-left diagonal, is not applicable due to the partial overlap of the transition region and additional minimum. This implies that the obtained one dimensional free energy profile (Figure S10.1 e) is not meaningful. The 1D profile indeed shows an intermediate free energy minimum around a CN1-CN2 value of zero, masking the real barrier for the direct methylation reaction.

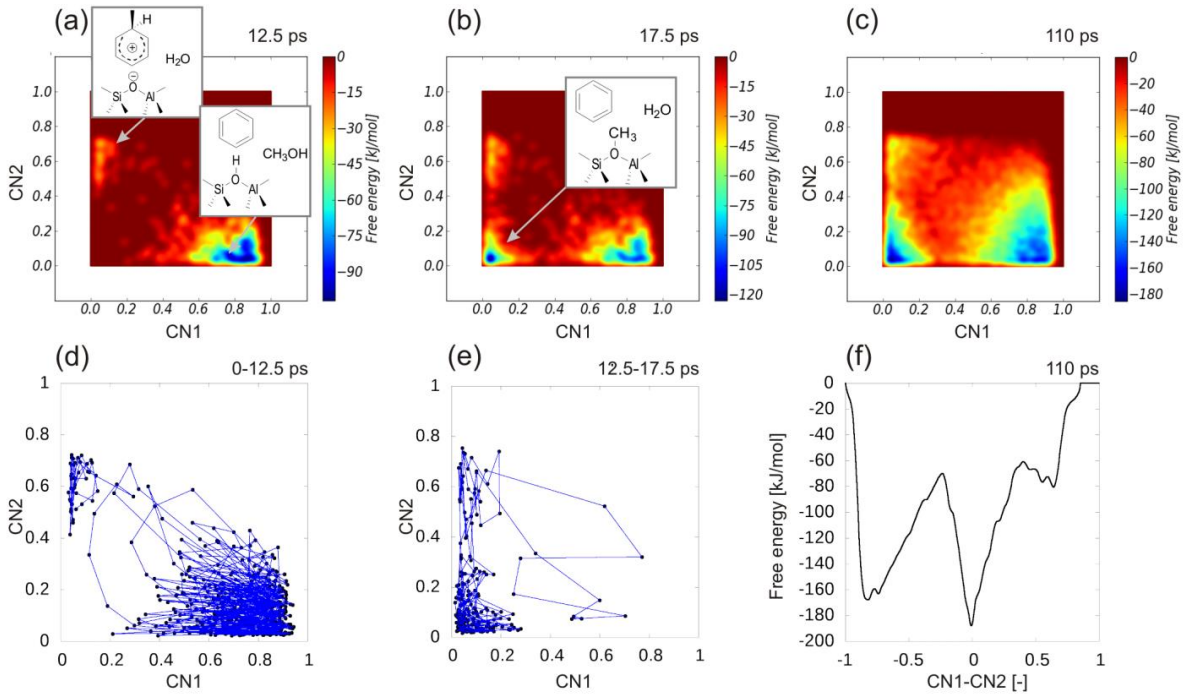

Figure S10.1. Two dimensional free energy maps for the methylation of benzene in H-SSZ-24 from a MTD simulation with 2 collective variables after (a) 12.5 ps, (b) 17.5 ps and (c) 110 ps; the corresponding sampled paths between 0-12.5 ps (d) and 12.5-17.5 ps (e) and the resulting one dimensional free energy profile after 110 ps as a function of CN1-CN2 (f).

S11. Additional computational details for the metadynamics simulations

Quadratic walls of the form K*(CV-position)^2 were used to restrict the simulations to a region of interest. Next to the active collective variables, two additional ones were introduced to describe the coordination of the methanol oxygen with the same methanol's hydrogen atom ($CN(O_m\text{-}H_1)$) and the acidic proton ($CN(O_m\text{-}H_2)$). For both additional coordination numbers the r_0 value was set to 1.0 Å. A brief overview of the applied quadratic walls and the characteristics of the spawned hills during the MTD simulations is given below.

a. Two dimensional simulation

Walls

- $0.04 \leq CN1$ with K = 50.0 hartree
- $0.03 \leq CN2 \leq 0.72$ with K = 15.0 hartree
- $0.03 \leq CN(O_m\text{-}H_1)$ with K = 100.0 hartree
- $0.03 \leq CN(O_m\text{-}H_2)$ with K = 100.0 hartree

Gaussian width and height

- CN1: width 0.02
- CN2: width 0.02
- Height is halved after recrossings: 4.82 kJ/mol – 2.4 kJ/mol – 1.2 kJ/mol

b. Three dimensional simulation

Walls

- $0.04 \leq CN1$ with K = 50.0 hartree
- $0.03 \leq CN2 \leq 0.72$ with K = 15.0 hartree
- No walls for CN3

- $0.03 \leq CN(O_m\text{-}H_1)$ with K = 100.0 hartree
- $0.03 \leq CN(O_m\text{-}H_2)$ with K = 100.0 hartree

Gaussian width and height

- CN1: width 0.02
- CN2: width 0.02
- CN3: width 0.02
- Height is halved after recrossings: 4.82 kJ/mol – 2.41 kJ/mol – 1.21 kJ/mol – 0.60 kJ/mol

S12. Sampled reaction pathways during a 3D metadynamics simulation of benzene methylation by 2 methanol molecules in H-SSZ-24 at 350 °C

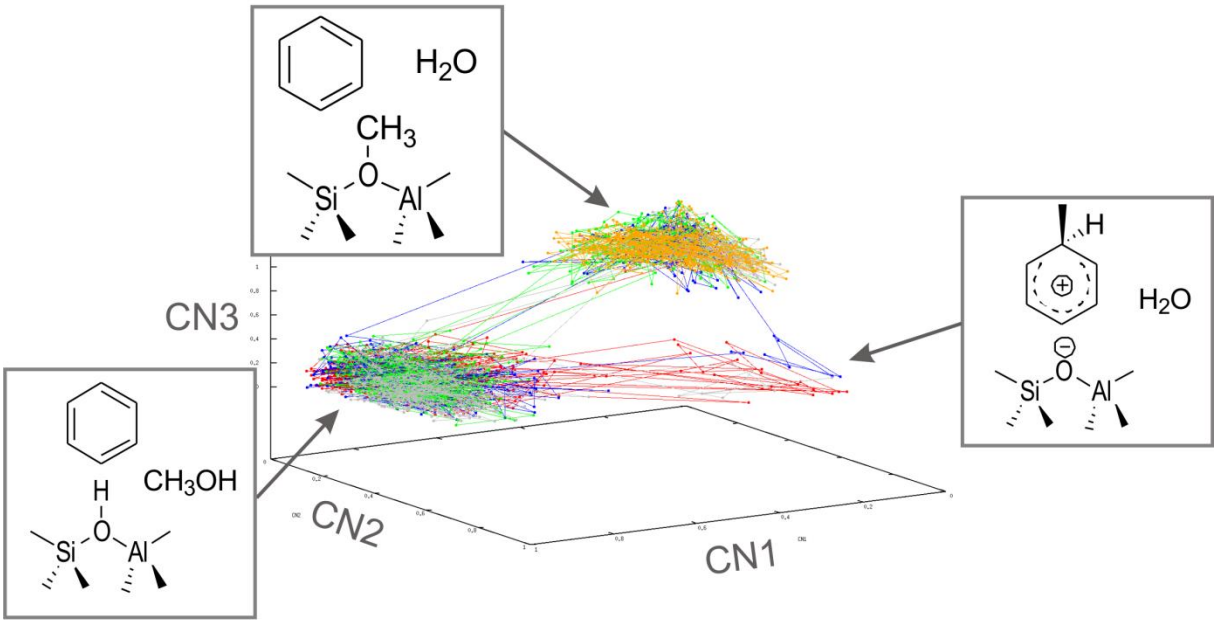

Figure S12.1. Paths sampled during the 235 ps MTD simulation with 3 CVs of the benzene methylation by two methanol molecules in H-SSZ-24 at 350 °C.

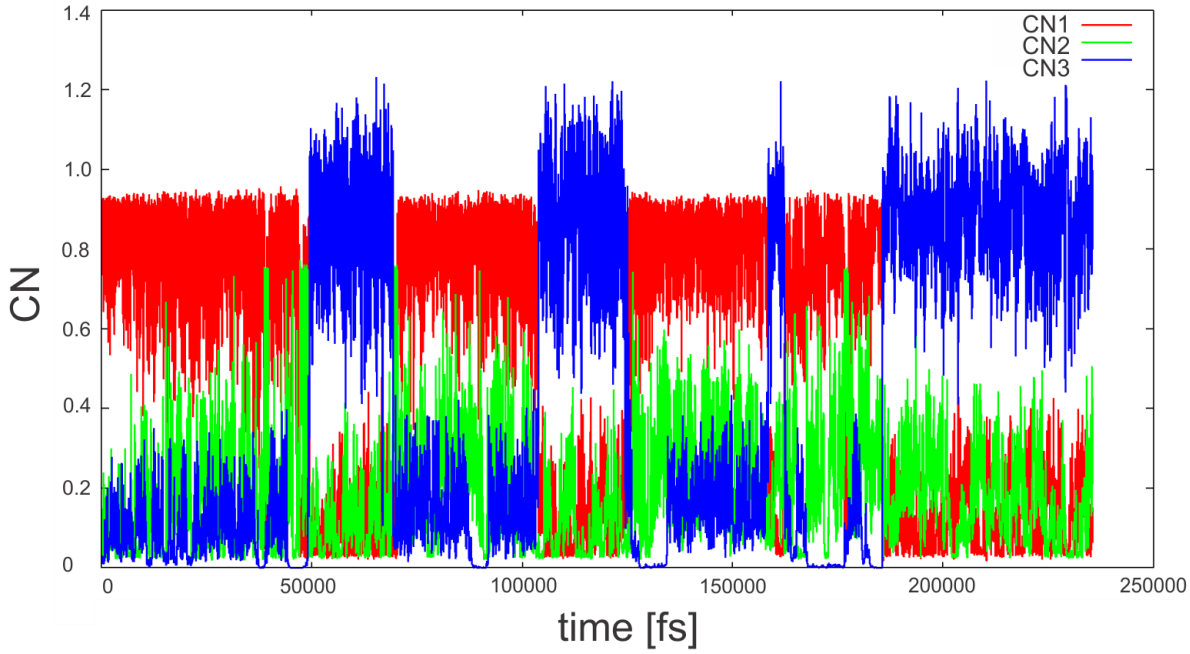

Figure S12.2. Evolution of the 3 collective variables during the 235 ps MTD simulation of the benzene methylation by two methanol molecules in H-SSZ-24 at 350 °C.

S13. Protonation of methanol during the 3D MTD simulation of benzene methylation by 2 methanol molecules in H-SSZ-24 at 350 °C

The methanol molecule that is a priori defined in the collective variables to undergo the methylation reaction or methoxide formation interacts with two hydrogen atoms: it has one hydrogen atom in the methanol OH group and interacts with a proton originating from the framework. To check how fast the protonation of methanol occurs, the methanol C-O bond length is plotted versus the largest of these two O-H distances (Figure S13.1). When the methanol molecule is still intact (d(Cm-Om) around 1.6 Å), both protonated and neutral methanol is present (the distances on the horizontal axis vary between 1.0 Å, indicative for protonated methanol, and 1.9 Å which is characteristic for a hydrogen bond). This region is indicated with the grey shaded area in the plot. When the methanol C-O bond starts to elongate, i.e. a reaction occurs (methylation or methoxide formation), the methanol molecule of course has to get activated by the acidic proton, which is clearly indicated by the fact that the values on the horizontal axis do not exceed 1.1 Å once the methanol C-O bond is broken (d(Cm-Om) > 2 Å). That the grey shaded area, representing the reactant state, contains both protonated and neutral methanol suggests that protonation and deprotonation of methanol occurs faster than the further reactions and does not substantially contribute to the activation barrier for these further reactions.

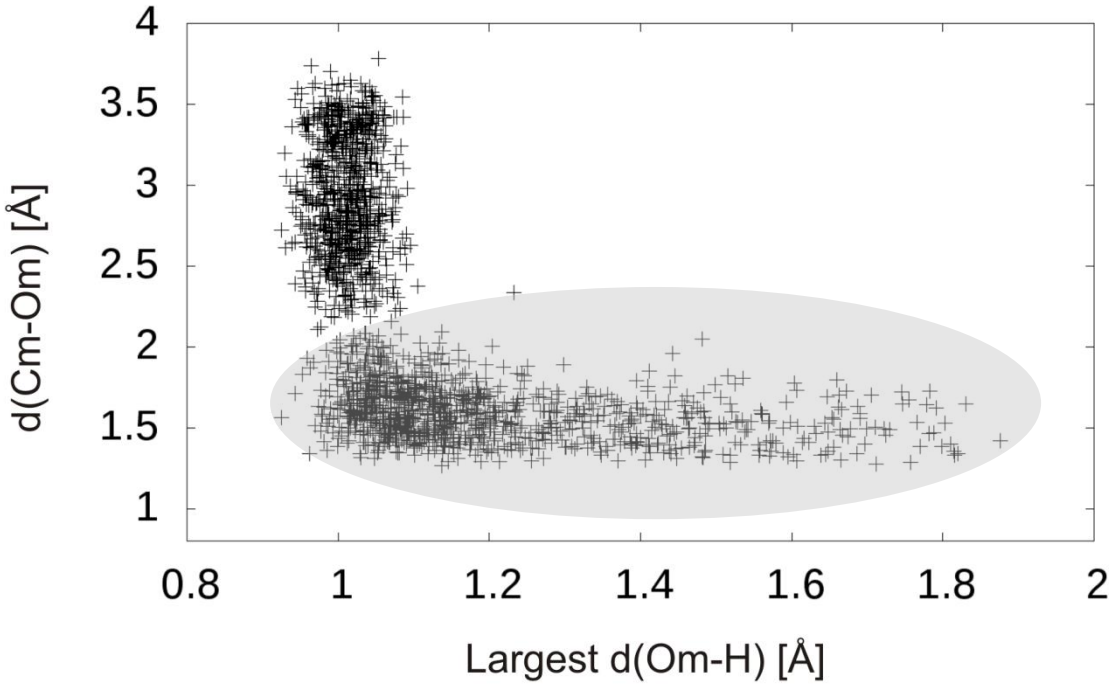

Figure S13.1. Methanol C-O bond length versus the largest methanol oxygen – acidic proton distance. Each point represents a configuration sampled during the 235 ps MTD simulation with 3 CVs of the benzene methylation by two methanol molecules in H-SSZ-24 at 350 °C.

S14. Role of the second methanol molecule during the benzene methylation by 2 methanol molecules in H-SSZ-24 at 350 °C

To get a notion of the importance of methanol – methanol interactions during the methylation of benzene with 2 methanol molecules, the C-O distance of the reacting methanol molecule is plotted versus the distance between the two methanol oxygen atoms. When the latter is smaller than 3.5 Å and the O-H ---O angle is well oriented, a hydrogen bond exists between the two methanol molecules. The highlighted area in Figure S8.1 indicates a high probability for methanol-methanol interactions when the reacting methanol molecule is intact. After reaction and thus formation of a water molecule (d(Cm1-Om1) > 2 Å), there is less preference for hydrogen bonding between the two protic molecules (water and methanol in this case).

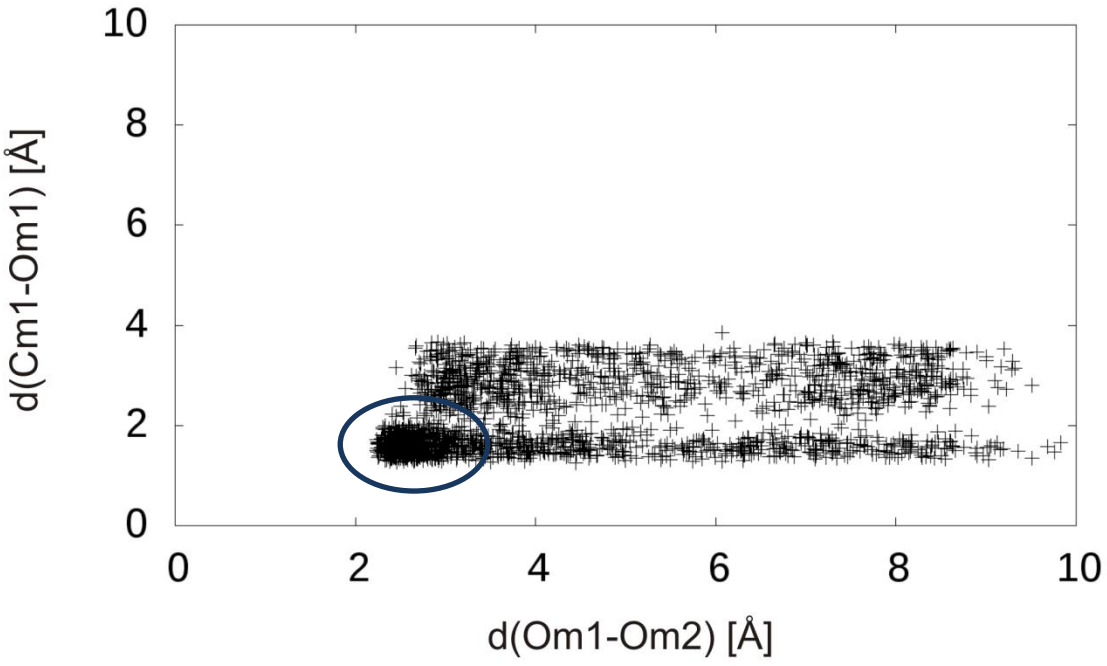

Figure S14.1. Methanol C-O bond length versus the largest methanol oxygen – acidic proton distance. Each point represents a configuration sampled during the 235 ps MTD simulation with 3 CVs of the benzene methylation by two methanol molecules in H-SSZ-24 at 350 °C.

S15. Free energy profiles along the lowest free energy paths for the benzene methylation by 2 methanol molecules in H-SSZ-24 at 350 °C

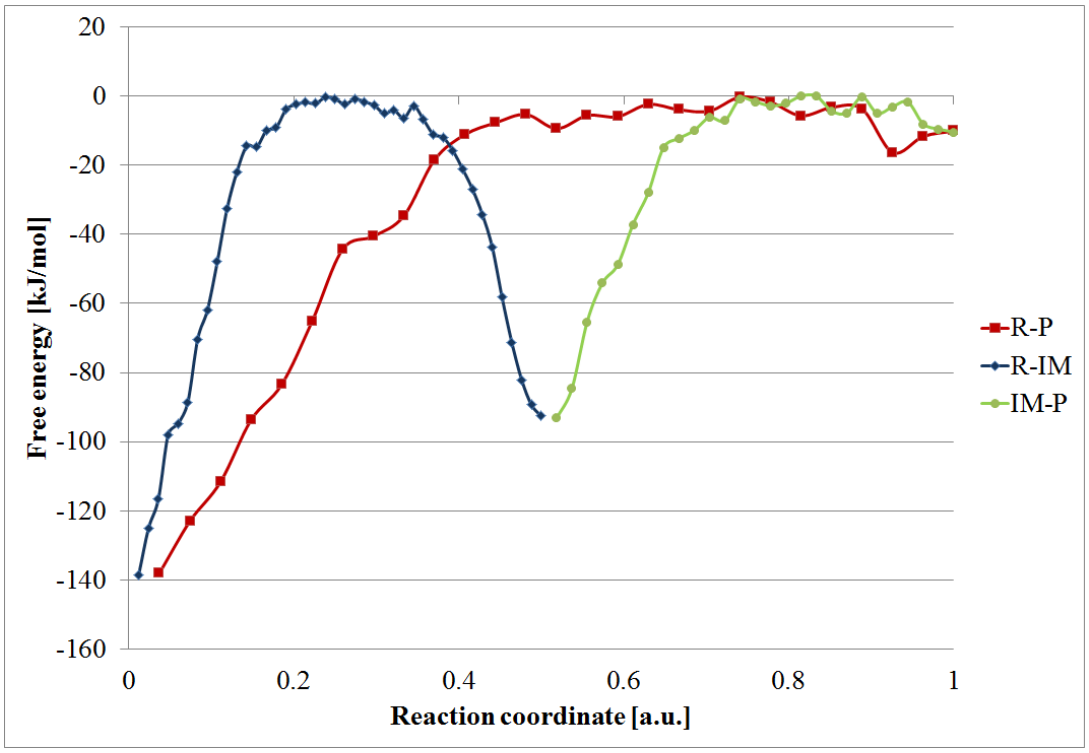

Figure S15.1. Evolution of the free energy along the reaction coordinate corresponding with the direct (R-P, red) and step-wise (R-IM in blue and IM-P in green) methylation of benzene in H-SSZ-24.

Convergence of the free energy profiles:

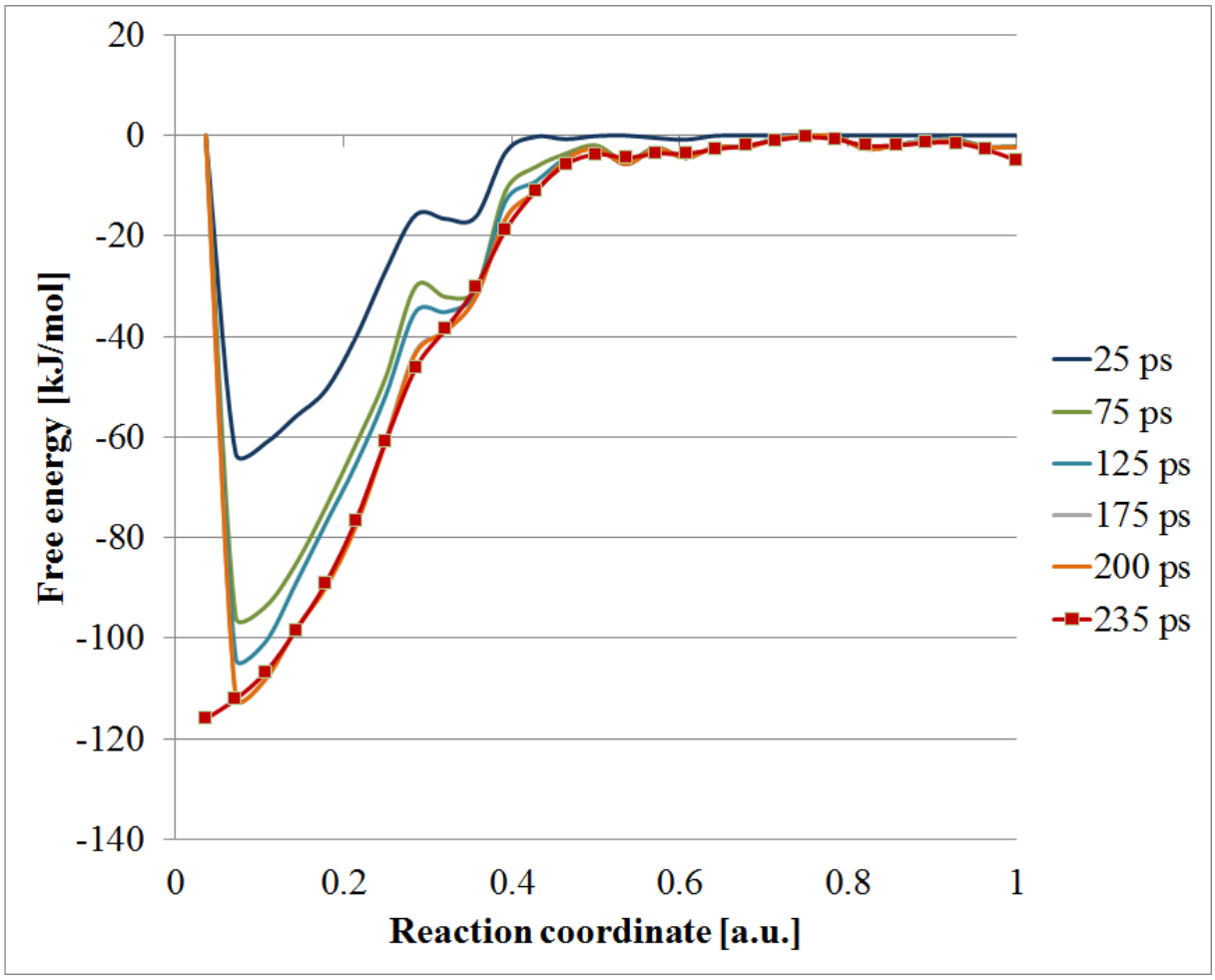

Figure S15.2. Lowest free energy path corresponding with the direct methylation of benzene by 2 methanol molecules in H-SSZ-24 at 350 °C after different simulations times.

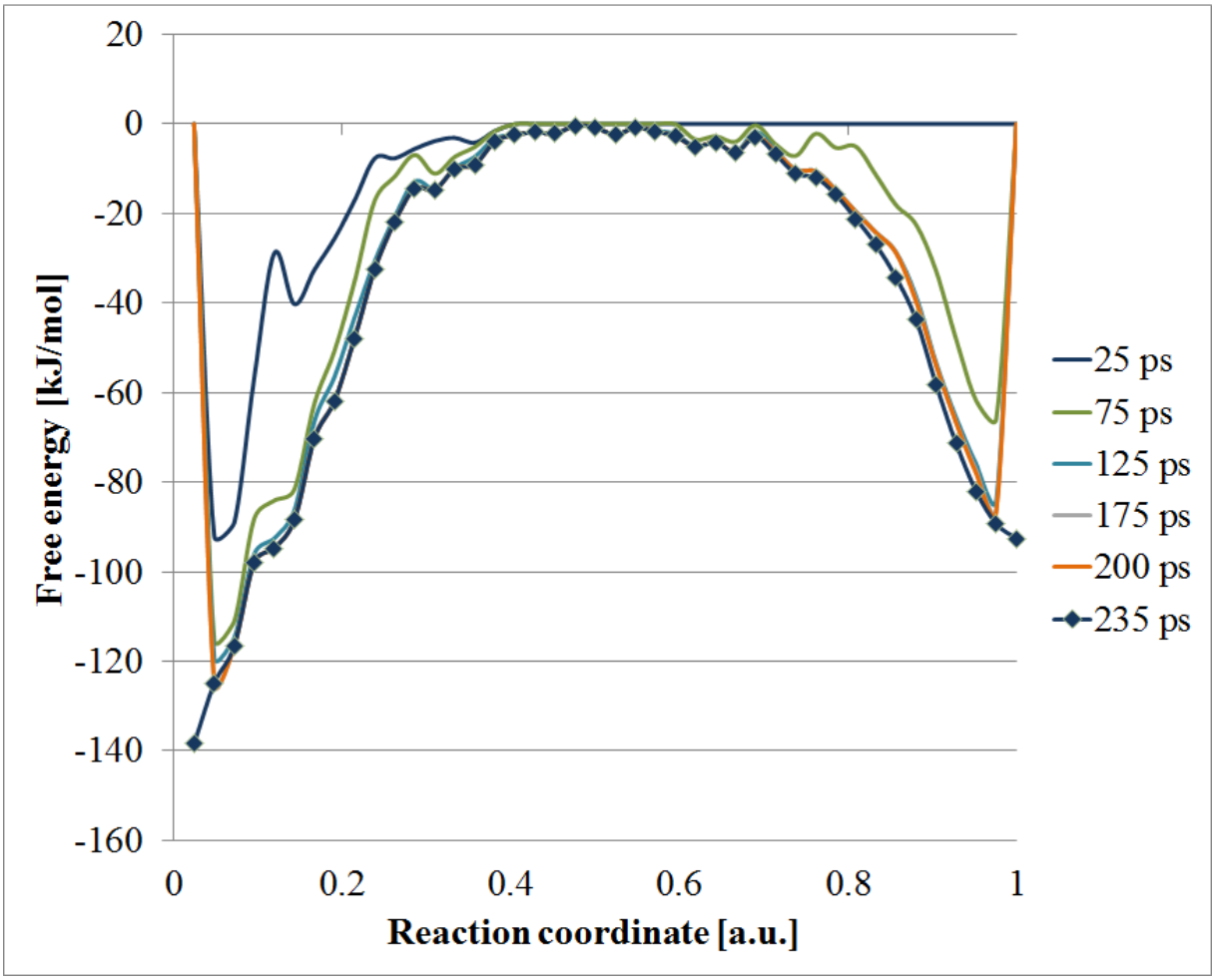

Figure S15.3. Lowest free energy path corresponding with the first step of the stepwise methylation of benzene by 2 methanol molecules in H-SSZ-24 at 350 °C after different simulations times.

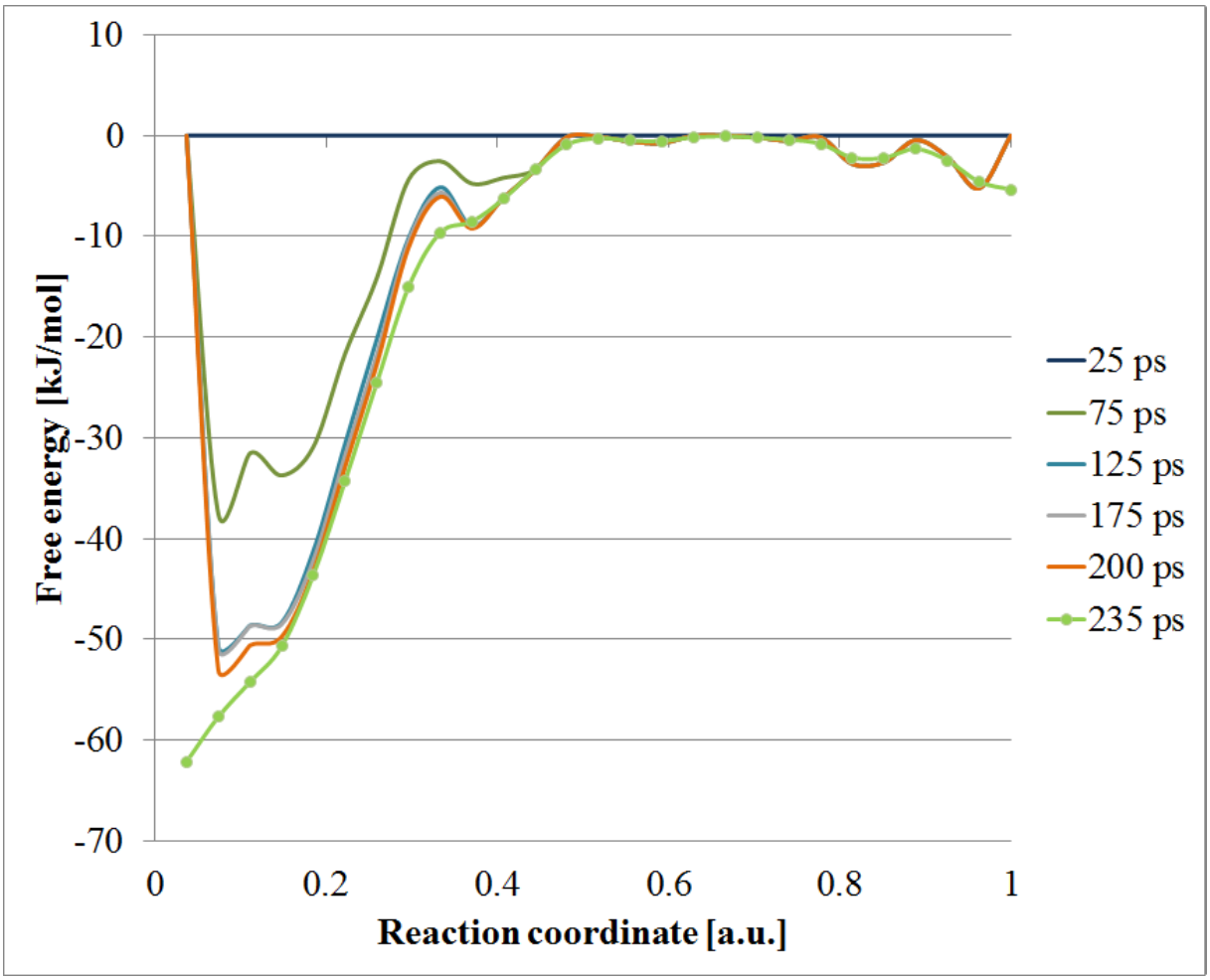

Figure S15.4. Lowest free energy path corresponding with the second step of the stepwise methylation of benzene by 2 methanol molecules in H-SSZ-24 at 350 °C after different simulations times.

References

[1] K. De Wispelaere, K. Hemelsoet, M. Waroquier, V. Van Speybroeck, *J. Catal.* **2013**, *305*, 76.
[2] K. Hemelsoet, A. Ghysels, D. Mores, K. De Wispelaere, V. Van Speybroeck, B. M. Weckhuysen, M. Waroquier, *Catal. Today* **2011**, *177*, 12.
[3] K. Hemelsoet, A. Nollet, V. Van Speybroeck, M. Waroquier, *Chem.-Eur. J.* **2011**, *17*, 9083.
[4] K. Hemelsoet, A. Nollet, M. Vandichel, D. Lesthaeghe, V. Van Speybroeck, M. Waroquier, *ChemCatChem* **2009**, *1*, 373.
[5] V. Van Speybroeck, K. Hemelsoet, K. De Wispelaere, Q. Qian, J. Van der Mynsbrugge, B. De Sterck, B. M. Weckhuysen, M. Waroquier, *ChemCatChem* **2013**, *5*, 173.
[6] V. Termath, F. Haase, J. Sauer, J. Hutter, M. Parrinello, *J. Am. Chem. Soc.* **1998**, *120*, 8512.
[7] G. Sastre, D. W. Lewis, C. R. A. Catlow, *J. Phys. Chem.* **1996**, *100*, 6722.
[8] M. Van Houteghem, A. Ghysels, T. Verstraelen, W. Poelmans, M. Waroquier, V. Van Speybroeck, *J. Phys. Chem. B* **2014**, *118*, 2451.
[9] D. Frenkel, B. Smit, *Understanding Molecular Simulations*, second edition ed., Academic press, Elsevier, **2002**.
[10] L. Sutto, S. Marsili, F. L. Gervasio, *Wiley Interdiscip. Rev.-Comput. Mol. Sci.* **2012**, *2*, 771.
[11] A. Laio, A. Rodriguez-Fortea, F. L. Gervasio, M. Ceccarelli, M. Parrinello, *J. Phys. Chem. B* **2005**, *109*, 6714.
[12] A. Laio, M. Parrinello, *Proc. Natl. Acad. Sci. U. S. A.* **2002**, *99*, 12562.
[13] B. Ensing, A. Laio, M. Parrinello, M. L. Klein, *J. Phys. Chem. B* **2005**, *109*, 6676.
[14] A. Laio, F. L. Gervasio, *Rep. Prog. Phys.* **2008**, *71*, 22.
[15] M. Iannuzzi, A. Laio, M. Parrinello, *Phys. Rev. Lett.* **2003**, *90*, 4.
[16] A. Barducci, M. Bonomi, M. Parrinello, *Wiley Interdiscip. Rev.-Comput. Mol. Sci.* **2011**, *1*, 826.
[17] J. Van der Mynsbrugge, S. L. C. Moors, K. De Wispelaere, V. Van Speybroeck, *ChemCatChem* **2014**, *6*, 1906.
[18] S. L. C. Moors, K. De Wispelaere, J. Van der Mynsbrugge, M. Waroquier, V. Van Speybroeck, *ACS Catal.* **2013**, *3*, 2556.
[19] V. Van Speybroeck, K. De Wispelaere, J. Van der Mynsbrugge, M. Vandichel, K. Hemelsoet, M. Waroquier, *Chem. Soc. Rev.* **2014**, *43*, 7326.
[20] S. Svelle, M. Visur, U. Olsbye, Saepurahman, M. Bjorgen, *Top. Catal.* **2011**, *54*, 897.
[21] M. Westgård Erichsen, K. De Wispelaere, K. Hemelsoet, S. L. C. Moors, T. Deconinck, M. Waroquier, S. Svelle, V. Van Speybroeck, U. Olsbye, *J. Catal.* **2015**, DOI:10.1016/j.jcat.2015.01.013.